Medical & Biological Engineering & Computing
https://doi.org/10.1007/s11517-024-03038-7

ORIGINAL ARTICLE

Influence of build orientation and support structure on additive manufacturing of human knee replacements: a computational study

Stephanie DeCarvalho[1] · Osama Aljarrah[2] · Zi Chen[3] · Jun Li[1]

Received: 13 January 2023 / Accepted: 29 January 2024

Abstract
Developing patient-specific implants has an increasing interest in the application of emerging additive manufacturing (AM) technologies. On the other hand, despite advances in total knee replacement (TKR), studies suggest that up to 20% of patients with elective TKR are dissatisfied with the outcome. By creating 3D objects from digital models, AM enables the production of patient-specific implants with complex geometries, such as those required for knee replacements. Previous studies have highlighted concerns regarding the risk of residual stresses and shape distortions in AM parts, which could lead to structural failure or other complications. This article presents a computational framework that uses CT images to create patient-specific finite element models for optimizing AM knee replacements. The workflow includes image processing in the open-source software 3DSlicer and MeshLab and AM process simulations in the commercial platform 3DEXPERIENCE. The approach is demonstrated on a distal femur replacement for a 50-year-old male patient from the open-access Natural Knee Data. The results show that build orientations have a significant impact on both shape distortions and residual stresses. Support structures have a marginal effect on residual stresses but strongly influence shape distortions, whereas conical support exhibits a maximum distortion of 18.5 mm. Future research can explore how these factors affect the functionality of AM knee replacements under in-service loading.

Keywords Finite element simulations · Residual stress · Shape distortion · Knee replacements · Additive manufacturing

1 Introduction

The knee joint is one of the body's most complex and stressed structures. A partial or total knee replacement (TKR) must reduce knee discomfort for severe knee osteoarthritis [1]. Today's knee implants have increased mobility, geometry, wear, and materials and coatings. To meet human knee features, bone fixation implants are most typically made of stainless steel (ISO 5832-1), cobalt-chromium-based alloys, and titanium (ISO 5832-2) as well as its alloys. These materials combine biocompatibility and functionality, although metallic implants may have stress-shielding or toxicity issues [2]. On the other hand, osteoclast-rigid implants can be made from carbon-reinforced composites [3]. Low-stiffness plastic implants often cannot perform biological or mechanical activities throughout time. Knee replacement performance depends on design and manufacturing [4]. Different knee implant hierarchies should match. Therefore, the implant should be strong enough to endure stress and allow blood flow [5]. Implant size and shape play a vital role in bone joint replacement design, and due to the complex knee geometry and design needs, additive manufacturing (AM) is emerging as a viable fabrication option.

In contrast to the traditional subtractive processes, AM is a technique to construct three-dimensional (3D) products

✉ Jun Li
jun.li@umassd.edu

Stephanie DeCarvalho
sdecarvalho@umassd.edu

Osama Aljarrah
oaljarrah@kettering.edu

Zi Chen
zchen33@bwh.harvard.edu

[1] Department of Mechanical Engineering, University of Massachusetts Dartmouth, 285 Old Westport Road, Dartmouth, MA 02747, USA

[2] Department of Industrial and Manufacturing Engineering, Kettering University, 1700 University Ave, Flint, MI 48504, USA

[3] Division of Thoracic Surgery, Brigham & Women's Hospital, Harvard Medical School, 75 Francis St, Boston, MA 02115, USA

Published online: 03 March 2024

by adding successive layers of materials, often in a sequential pattern, based on digital model [6, 7]. AM can create parts of almost any complicated geometry with a broad range of design flexibility and material attributes [7–9]. Although AM technology is burgeoning, several possible issues exist before production use [10]. Considering that AM involves a layer-upon-layer process of heating and cooling, the structural integrity of an AM component may be compromised. A 3D-printed product could have quality issues such as residual stresses, shape distortions, microstructural defects, porosity, and dimensional stability. Nevertheless, the advantages of AM have paved the way for the development of biomedical products [11–14]. In particular, the potential applications of AM in patient-specific implants are exciting because of its capability to adapt to the environment of its intended use [15].

Computed tomography (CT)-derived 3D human body structures use quantitative CT images to build patient-specific finite element (FE) models. CT-FEM models can determine the reaction of a structure to external forces and thus predict the deformation, stress distributions, and evaluate failure [16–18]. Moreover, CT-FEM platforms can be used for further evaluations in AM quality [19]. Zeng et al. [16] built a computational FE model for scapular mechanics using musculoskeletal information extracted from CT scans of a female subject. Risk patterns of bone failure were then examined using three standard failure metrics [20].

Regarding AM medical implants, Jahadakbar et al. [21] recommended using superelastic NiTi, whose stiffness matches that of a cortical bone. They developed FE models to assess the effectiveness of the suggested NiTi fixation. They found that stress is distributed more uniformly with reduced contact stress at the bone graft interface using the Ti-6Al-4V off-the-shelf fixation hardware. Zhao et al. [22] studied biocompatible femur bone scaffolds by fused deposition modeling the AM process. They employed a polymer composite material of polyamide, polyolefin, and cellulose fibers for medical purposes. Consequential process parameters were applied using a cascade technique followed by Taguchi design for process optimization experimentally. Computational FE models were also developed to investigate the physical processes behind the experimental findings. Cheng et al. [23] utilized topology optimization to minimize the volume of a sacrificial support structure while considering stress constraints. After optimization, the support structure can achieve a weight reduction of around 60% and also avoid residual stress-induced build failure.

According to Beswick et al. [24] and Wylde et al. [25], 10–34% of knee replacement patients report long-term discomfort after the surgery. The advancement in AM allows the creation of a patient-specific knee implant from CT scans for greater long-term mobility and comfort. However, the residual stresses and shape distortions caused by the AM process could significantly impact mechanical performance and reduce knee replacement success rates. Although previous studies used CT scans as non-destructive tests to evaluate AM parts [26], the quality performance of an AM part can also be assessed using computational simulations.

With an emphasis on reducing residual stresses and shape distortions, this study attempts to determine the most critical additive manufacturing (AM) configuration for patient-specific knee replacements. We evaluate the quality performance of AM components using thermo-mechanical finite element simulations with respect to pre-specified 3D printing settings. This method reduces costs and increases efficiency by anticipating problems before they arise during testing. Consequently, the research question is crafted to outline variations in residual stresses and distortions among distinct additive manufacturing configurations tailored for individualized knee replacements. This investigation seeks to establish the impact of these variations on the efficiency and reliability of additively manufactured knee replacements. Accordingly, integrating simulation-based assessments in additive manufacturing becomes instrumental in mitigating distortions and residual strains, enabling the early identification of potential issues.

2 Methods

2.1 Method overview

A comprehensive computational workflow is developed from the design to additive manufacturing of patient-specific knee replacements using CT images and FE simulations. The workflow begins with the creation of a 3D knee model based on CT images, which are from a 50-year-old human male donor of an open knee database at Denver University's Center for Orthopaedic Biomechanics [27, 28]. The overall workflow is depicted in Fig. 1.

A DICOM (Digital Imaging and Communications in Medicine) file containing compressed images was used to set up the model. The open-source software 3DSlicer [29] was employed for image segmentation and reconstruction, converting the DICOM data into a 3D model. Specifically, the femoral knee was selected in this study. The resulting STL geometry file of the femoral bone was created using the open-source software MeshLab [30], which involved image filtering and smoothing. Finally, commercial software 3DEXPERIENCE [31] was utilized to simulate the selective laser melting (SLM) [32] AM process for the knee replacement model. Sections 2.2 and 2.4 provide more detailed procedures on transforming CT images into 3D FEM models and setting up AM simulations, respectively. The Table below 1 shows the list of software utilized in this research.

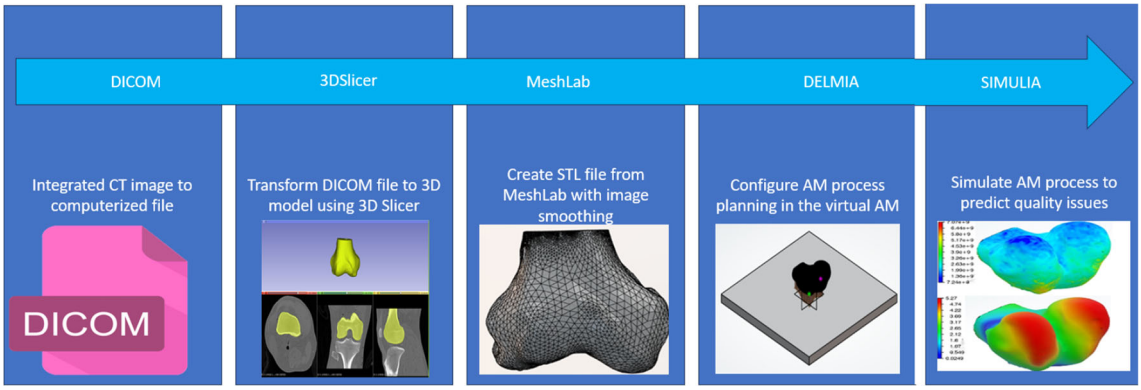

Fig. 1 The overall workflow from CT images to 3D models and AM simulations

The knee replacements were virtually additively manufactured using selective laser melting (SLM), a technique known for its effectiveness in creating porous bone implants, including knee implants [33]. The 3DEXPERIENCE platform houses a couple of simulation applications (APPs) that integrate with one another to form a cohesive and seamless work environment from design to analysis and manufacturing [34]. During the simulation, a sequence of events follows the printing trajectory, where element activation occurs to mimic the underlying physical process of additive manufacturing [35, 36]. It should be noted that rigorous theoretical and experimental verification and validation have been performed on the 3DEXPERIENCE platform for simulating various materials and AM processes, including SLM [37–39]. In this study, we focus on simulation-based research that provides insights into the optimal build orientation and support structure for AM knee replacements. Further experimental validations and clinical evaluations will be considered in future research.

The AM simulation involves two consecutive APPs in 3DEXPERIENCE: the first is DELMIA Powder Bed Fabrication (PBF) APP, in which the machine and build substrate establish the simulation domain (see Fig. 2), and the model defines the FE computational field. Build orientation, support structure, scanning speed, layer thickness, cooling rate, laser energy, and all other process parameters for the build strategy can be defined in the PBF APP [40]. The build substrate is assumed to be rigid and maintain a constant temperature at the bottom. The PBF APP also defines the airflow. The control variables include the temperatures of the build substrate and the ambient air. The second is SIMULIA Additive Manufacturing Scenario Creation (AMSC) APP. A moving volume source is used to define the laser in the additive manufacturing process [41]. Moreover, a user material definition APP can be specified to define the temperature-dependent material properties and powders thermal characteristics [42, 43] for high-fidelity simulations.

2.2 Transforming the CT scans into a finite element model

To ensure accurate knee replacement modeling, CT data from Natural Knee Data (NKD) at Denver University [27, 28] was gathered, featuring detailed information for five patients aged 37 to 72 years and weighing 54 to 127 kg. The selected patient, a 50-year-old male (175 cm, 127 kg), had DICOM files, retrieved from NKD, imported into 3DSlicer [29] for 3D modeling.

In 3DSlicer, a specific segment representing the region of interest was chosen and processed to isolate bones from surrounding tissues using the threshold function. Manual editing and cleanup were performed, as depicted in Fig. 3. The resulting 3D femur model was exported as an STL file to MeshLab [30] for additional filtering and smoothing. The refined model was then imported into ABAQUS [44] for finite element simulations. ABAQUS, equipped with a mesh-to-geometry plug-in, transformed the femur mesh into a solid body, facilitating subsequent simulations.

The finalized model was exported as an SAT file from ABAQUS and imported into the 3DEXPERIENCE platform [31] for additive manufacturing simulations. Further details

Table 1 List of software used in the research

Software	Year	Version	Company	Open-source
3DSlicer	2019	5.4	Ultimaker Cura	yes
MeshLab	2020	2020.12	ISTI - CNR	yes
3DEXPERIENCE	2023	2023x	Dassault Systèmes	No

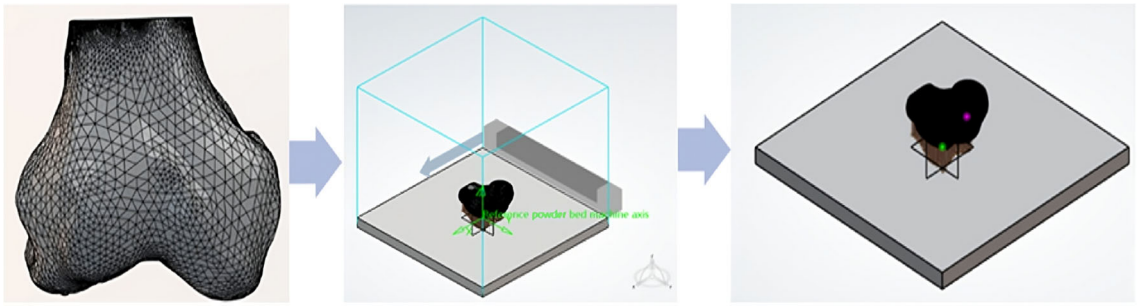

Fig. 2 Stages of additive manufacturing (AM) simulations in 3DEXPERIENCE platform: **a** Material Definitions APP to assign temperature-dependent material properties on FE models; **b** Powder Bed Fabrication APP to define AM machine process parameters such as substrate and tool-trajectory; **c** Additive Manufacturing Scenario Creation APP, which performs thermo-mechanical FE simulations for AM process

about the finite element model are provided in the results section during the mesh convergence study.

2.3 Process planning of additive manufacturing

A number of process parameters can influence the quality of AM parts. Both shape distortions and residual stresses induced by AM processes are investigated in this study as main potential sources of reduced part quality [45]. We focus on two key configurations in the AM process planning: build orientation and support structure. Parametric studies by varying those configurations will be performed to investigate their effects.

Three different build orientations are evaluated on the knee model, numbered 1–3 for ease of reference, as shown in Fig. 4. To investigate accurately how each configuration affects the part quality, all other parameters would remain constant while changing a single aspect of the model. The baseline model that is referred to as the "standard" in this scenario is the build Orientation 1. This was chosen because it has the largest flat surface for the support structure to be attached to. Besides, it does not require as much height, which could lead to a more efficient printing process. One major issue of the PBF technique is the occurrence of overhanging features during laser processing. This may drastically limit the geometries that the processes could produce, increase production time and cost, and affect part quality since components may not be conveniently stacked in the build bed, which requires support structures for AM parts [46].

The 3DEXPERIENCE DELMIA PBF APP offers three different types of support structures to choose from: wired (anchor), conical, and tree supports, as shown in Fig. 5. In wired (anchor) support, anchor columns generate anchored material connections between the build tray and printed part using a model material. The anchor columns prevent part-lifting and curling and often provide a more firm connection than the usual bed of support material. Conical supports, on the other hand, provide an angled support structure in

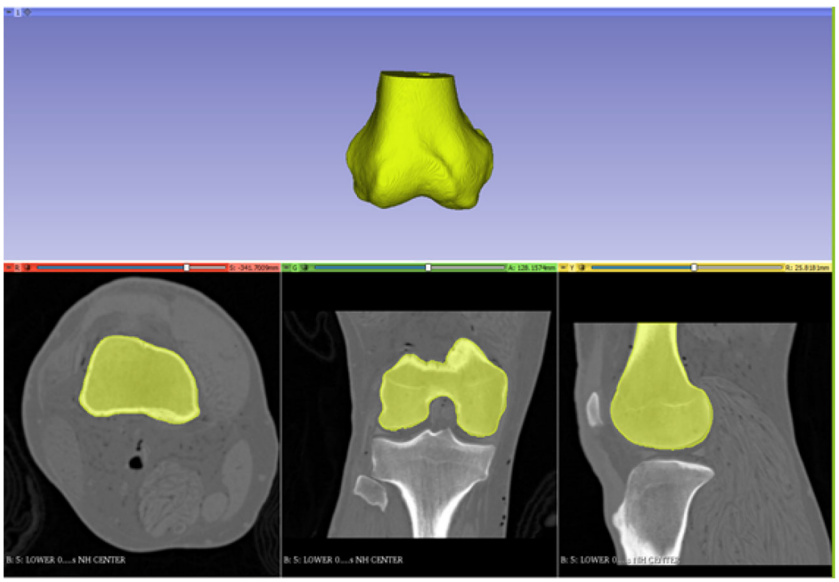

Fig. 3 Image segmentation and visualization of the femur model in 3DSlicer

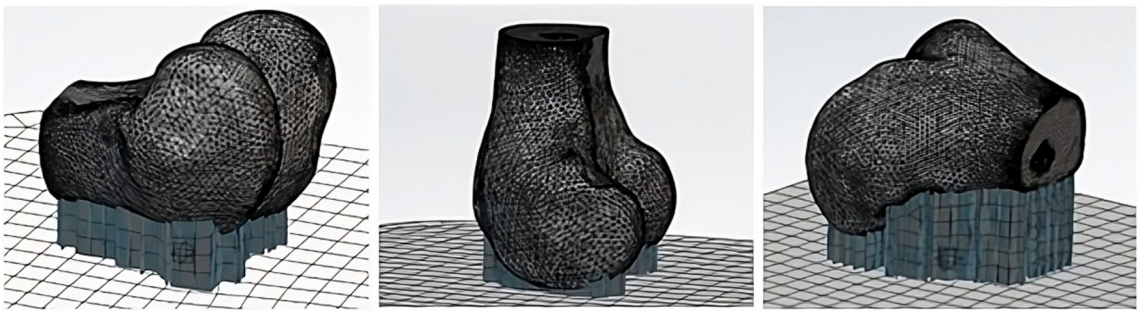

Fig. 4 Different build orientations for the knee model: Orientation 1 (**left**), Orientation 2 (**middle**), and Orientation 3 (**right**)

a cone shape that grows smaller or bigger toward the bottom. Finally, the tree supports appear to be composed of "trunk" and "branches," mimicking the organic structure of a tree. The major advantage of tree supports is that they do not contact the print on as many surfaces as other supports, resulting in a much cleaner final print [47]. The base support structure used during the AM simulations was the anchor support, which is the simplest and most commonly used type of support structure in practice.

2.4 Configuring the additive manufacturing simulations

The additive manufacturing simulations are performed on the commercial 3DEXPERIENCE platform [31], which integrates computer-aided design, manufacturing, and engineering analysis (CAD/CAM/CAE). First, the femur model created from CT scans in Section 2.2 was imported into the 3DEXPERIENCE, in which the Material Definitions APP was used to assign material properties. Since most biomedical implants are made of titanium aluminum or cobalt-chromium alloys, the material chosen is medical-grade titanium of Ti-6Al-4V [48] suitable for additive manufacturing. The material is assumed to be isotropic with thermal and mechanical properties listed in Table 2. Figure 6 shows the 3D femur model in the 3DEXPERIENCE platform from different perspectives.

Once the material properties were assigned to the part, the Powder Bed Fabrication (PBF) APP was then used to define settings for the additive manufacturing processes. Figure 7 shows the femur model in the PBF app. A simple machine and substrate (build tray) were created around the part based on the size of the femur. The layout of the part was arranged according to the build orientation. After that, the support structure was generated in the PBF APP based on the positioning of the part. The type of support structure can be chosen between wired (anchor), tree, and conical supports. The scan path generation was then defined, including the layer thickness, print speed, and laser power. The model defined in the PBF APP was then applied in the Additive Manufacturing Scenario Creation (AMSC) APP to perform FE simulations.

The AMSC APP creates a sequentially coupled thermal-mechanical analysis to simulate the additive manufacturing process. The simulation begins with a thermal analysis step and the temperature fields obtained at each time increment will then drive a mechanical analysis step, using material properties and thermodynamic laws to compute the corresponding thermal expansion/shrinkage, shape distortions, and residual stresses to the AM part. For convenience, the part material properties of Ti-6Al-4V were also applied to the support structure and the build tray. Tetrahedral meshes were applied to the part model. Tie constraints were used between the part, build tray, and support structure. After that, the melting temperature, chamber temperature, thermal absorption,

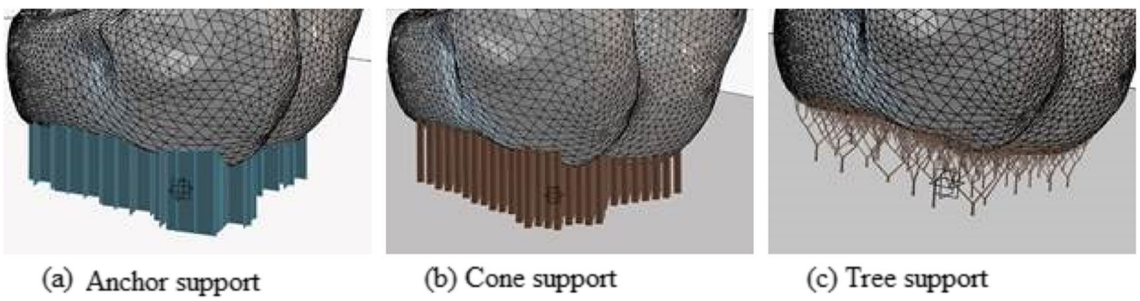

Fig. 5 Different types of support structures defined in 3DEXPERIENCE DELMIA PBF APP: **a** Anchor, **b** conical, and **c** tree

Table 2 Ti-6Al-4V thermal and mechanical properties

Density (kg/m^3)	4429	Thermal expansion coefficient ($/K$)	9×10^{-6}
Poisson's ratio	0.31	Thermal conductivity ($W/(m \cdot K)$)	6.7
Young's modulus (GPa)	104.8	Specific heat ($J/(K \cdot kg)$)	586.04

emissivity, and other crucial parameters were defined for the AM simulations to run. The AM process parameters are listed in Table 3. Structural restraints of boundary conditions are then assigned to the model, clamping the bottom of the build tray and fixing restraints on the support structure. Finally, the sequentially coupled thermal and structural simulations were performed, and the results were gathered.

3 Results

3.1 Mesh convergence study

A mesh convergence study was performed first to determine the appropriate mesh size for the knee model to ensure reliable results. Five mesh variations of the baseline AM model (Build Orientation 1 with wired supports) were run using meshes from 5 mm down to 1 mm on the AM part. The results of residual stresses and shape distortions were compared to verify the mesh convergence. Figures 8 and 9 show the final field contour plots of residual stress and shape distortions, respectively. Only results on the AM part (knee model) are displayed while the support structure and build plate are not shown as the latter two are not the region of interest. The results show that the mesh converged at 2 mm, and that was the size chosen in this study to ensure both accuracy and efficiency. The 1 mm mesh size was not chosen as the simulations took significantly longer than those with a 2 mm mesh size while the final results did not vary significantly.

3.2 Study of build orientation and support structure

Many studies showed that the AM part quality could be significantly influenced by PBF process parameters, such as powder layer thickness, hatch distance, laser power, and scan speed [49–51]. Note that the knee model has complicated geometry. In this study, we chose to investigate the geometric aspect of build orientation and support structure and how they affect the printed part quality. Figure 10 shows the final results of residual stresses and shape distortions from AM process simulations, in which the build orientation was altered. Other process parameters, such as the layer thickness, scanning speed, laser power, and hatch distance, listed in Table 3, were the same in all of these simulations so as to study the effects of build orientation. Build Orientation 1 was laid out such that the largest and flattest surface would be built touching the supports. Build Orientation 2 was specified as printed in the same orientation as it would be located in the body during loading. Build Orientation 3 has the largest surface area touching the support structure underneath it. The peak values of residual stresses and shape distortions in the AM knee model from AM process simulations for each build orientation are listed in Table 4.

Figure 11 shows the final simulation results of residual stress and shape distortion fields for the AM knee part when varying the types of support structures, with the corresponding peak values for each case listed in Table 5. It is pertinent to note that the simulations for conical and tree supports were more challenging due to their complicated geometries, which called for a voxel mesh of support structures instead of the typical tetrahedral mesh. As refined meshes would take much longer simulation time and cause difficulties in convergence, a coarser voxel mesh was applied to the support structures than was desired, which may affect the simulation accuracy, and this will be investigated in future research.

4 Discussion

The CT-FEM workflow was developed to predict residual stress and shape distortions in AM knee replacements, which

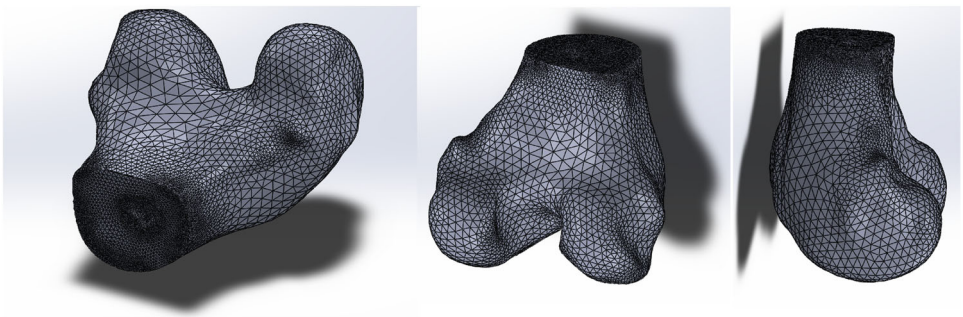

Fig. 6 Femoral model shown in 3DEXPERIENCE platform with different views

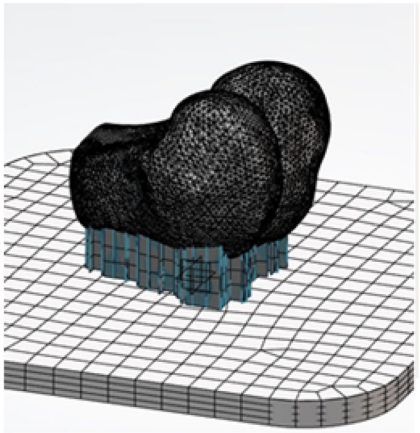

Fig. 7 Femur in Powder Bed Fabrication preparation app, laid in build orientation with the support structure

provides insights into the influences of build orientation and support structure through simulation-based parametric studies. A 3D knee model with complicated geometries is able to be created from its CT images in an open-access knee database. The open-source software 3DSlicer was used to generate a 3D model from a stack of 2D sliced CT images. The 3D model was further processed in the open-source software MeshLab with filtering and smoothing to be better prepared for finite element modeling. Finally, commercial software 3DEXPERIENCE was employed to configure and perform additive manufacturing process simulations of the 3D knee model.

Figure 10 illustrates how the build orientation of additive manufacturing affects the residual stresses and shape distortions of the knee replacement, with the corresponding peak values listed in Table 4. The build orientation with the greatest peak residual stress is Orientation 2, whereas the one with the lowest peak residual stress is Orientation 1. In Orientation 2, the peak stress of 10.3 GPa was located along the bottom of the femoral condyle, where the model is in direct contact with the support structures. This is likely the effect of a thin and small portion of the part being printed, which was heated and cooled repeatedly due to the nature of additive manufacturing, causing higher residual stress in this location. As each layer was simulated, the part was increasing in size, forcing the previous layers to adhere to the new layer's geometric constraints when the heating and cooling process promoted the shrinking of the material. Orientations 1 and 3 have similar locations for their peak stresses along the sharp edges on the cut plane of the femur. This location is expected due to the geometric constraints at these points, along with the process of the heating and cooling of each layer, causing residual stresses to be higher. The stresses found in each simulation are significantly higher than the yield strength of Titanium. This can be attributed to the default parameters used for the support structures. When support structures are very thin, the printing process is likely to result in higher stresses in the part. These high values of residual stresses could be reduced by increasing the thickness of support structures, adding fillets to printed parts, and/or introducing plasticity and yielding of the material in the simulation process. Orientation 2 displays lower peak shape distortions compared to the other two orientations. This can be attributed to the fact that it is constructed with no significant variances in the model jutting out or sharp angles that would be perpendicular to the printing process, as Orientation 3 does.

Figure 11 and Table 5 show the FE simulation results of residual stress and shape distortions for the knee replacement when varying the types of the support structure. Comparing the three different types of supports, it can be found that the residual stress distributions for all of them are somewhat similar, while the shape distortions are significantly different. This is likely due to the varying amount of support applied to different areas of the model by each type of support structure. It is interesting to note that the peak residual stresses of all three different supports do have some differences, with the wired one being in between the others. However, the maximum shape distortion that occurs as a result of altering the supports is what makes a large difference in this scenario. The peak shape distortions vary greatly among the three types of support structures, with the tree supports being about two times the wired supports and the conical supports being about three times the wired ones. The wired (or Anchor) support structure appears to be the optimal choice for minimizing shape distortions.

This study has several possible avenues to be extended in future work. With a complete workflow set up from CT images to 3D finite element models and additive manufacturing simulations, the effects of more process parameters (e.g., layer thickness, hatch distance, laser power, and scan speed) on AM part qualities as well as the interactions between different process parameters can be investigated through a large number of FE simulations and statistical ANOVA analysis. The predictions of residual stresses and shape dis-

Table 3 Additive manufacturing baseline process parameters

Laser power (W)	200	Melting temperature (K)	1940
Layer thickness (μm)	50	Chamber temperature (K)	1023
Scan speed (mm/s)	500	Convection coefficient ($W/(Km^2)$)	18
Absorption	0.5	Emissivity	0.45

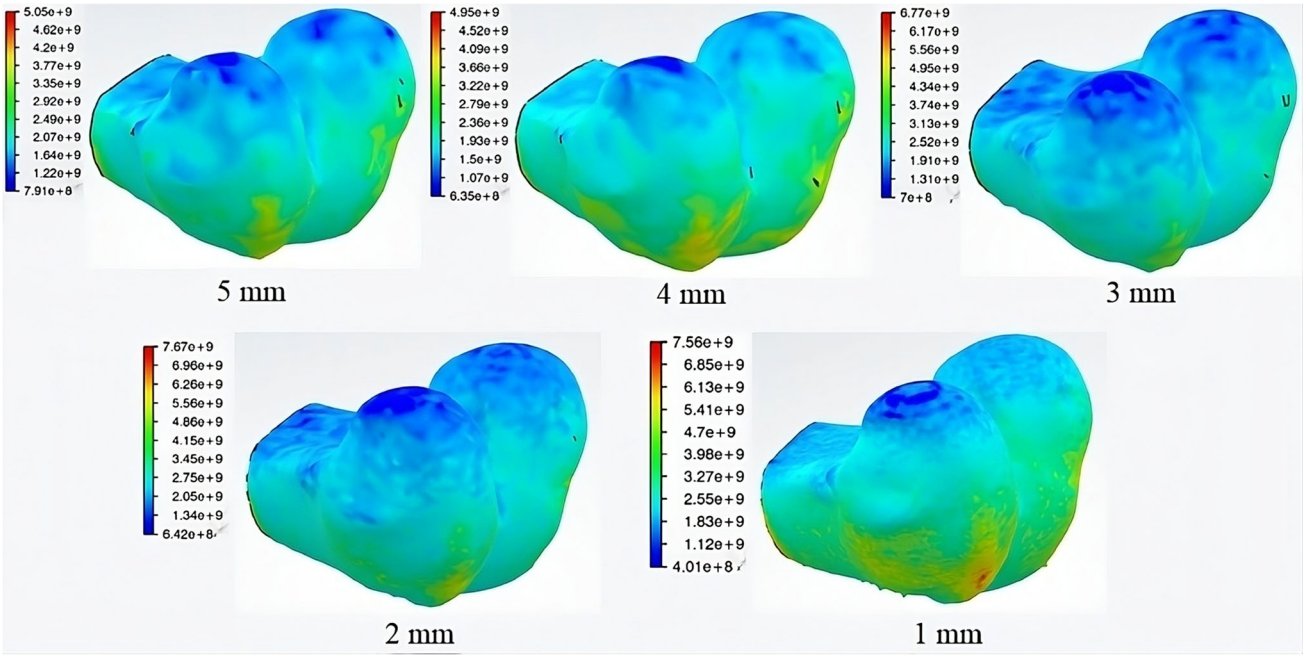

Fig. 8 Mesh convergence study on the baseline AM model (Build Orientation 1 with wired supports): comparison of residual stresses (unit: Pa) at varying meshes

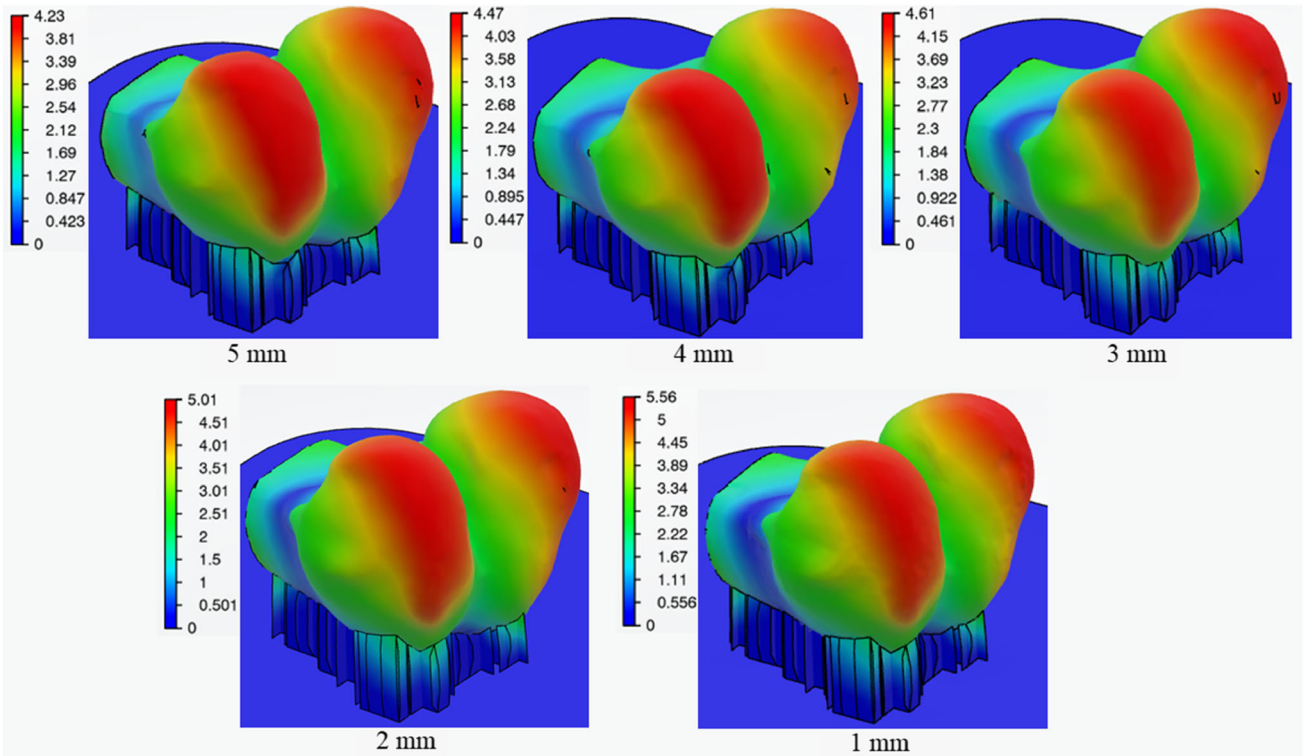

Fig. 9 Mesh convergence study on the baseline AM model (Build Orientation 1 with wired supports): comparison of shape distortions (unit: mm) at varying meshes

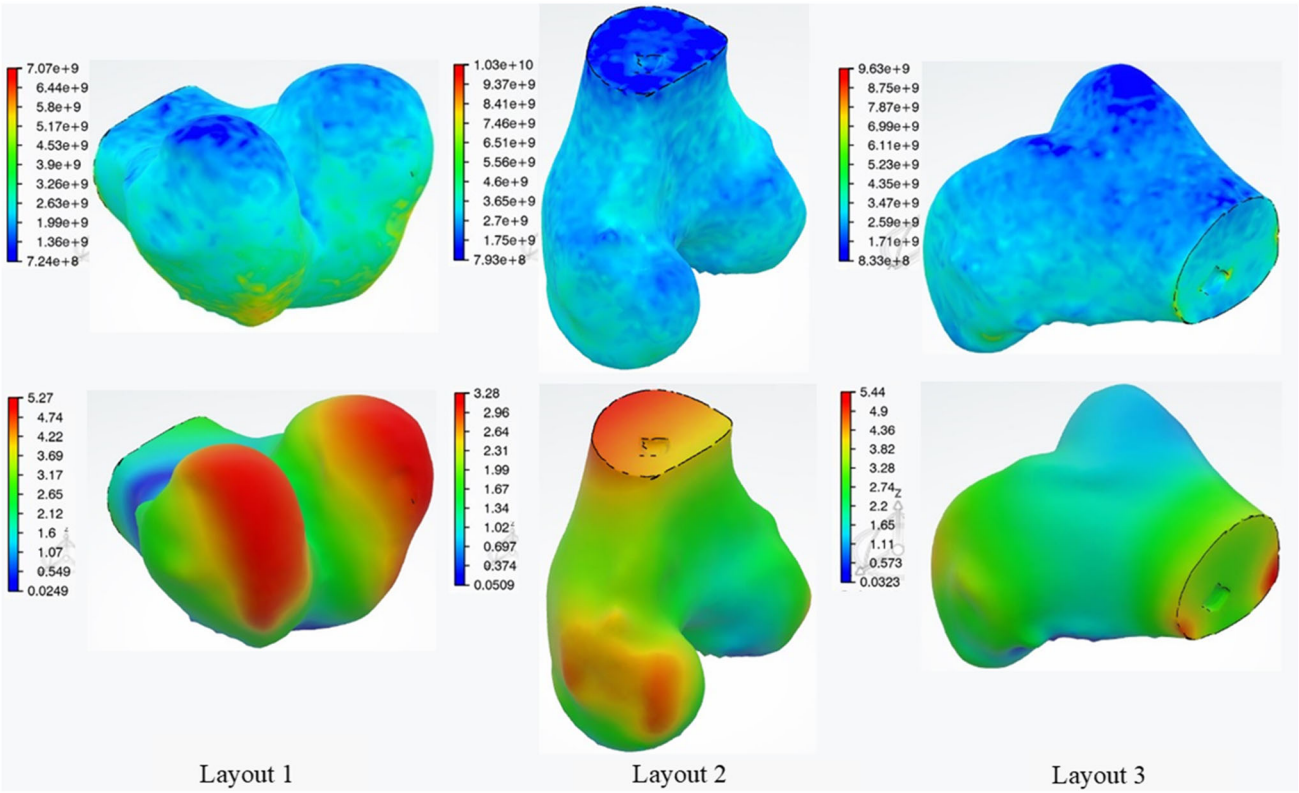

Fig. 10 Residual stress (top, unit: Pa) and part distortion (bottom, unit: mm) of the knee model, from AM simulations using three different build orientations: Orientation 1 (left), Orientation 2 (middle), and Orientation 3 (right)

tortions can be validated experimentally. It is pertinent to note that the 3DEXPERIENCE Additive Manufacturing simulation platform has been validated for residual stress and shape distortions against experimental measurements in [52, 53]. However, the knee structure has complicated geometries, which may bring enormous challenges in experimental measurements. Some conformal mapping-based surface registration methods for complicated surfaces could be useful in this regard [54]. Eventually, the physiological loading of knee joints can be considered on AM knee parts to evaluate the in-service performance of as-manufactured models with initial residual stress and shape distortions.

We note that the layered construction in the AM process could result in directionally cemented microstructures. The wear and corrosion resistance may be affected due to the anisotropic surface patterns [55], which can be implemented and optimized in future work. The simulation assumes that the part is fabricated entirely without cracking or delamination. During the AM process, intermediate and greater residual stress could be generated by the temporary steep heat gradient, which may cause delamination failure during printing. The study does not take into account the post-removability of support structures via machining. These issues can be studied more in the future in order to fully use simulations to improve part quality and support post-removal for existing powder bed fusion AM methods in practice.

Table 4 Peak values of residual stress and shape distortion in AM knee model when varying build orientations

Configuration	Max stress (GPa)	Max distortion (mm)
Orientation 1	7.07	5.27
Orientation 2	10.3	3.28
Orientation 3	9.63	5.44

While the use of a complete distal femur as a feasibility model is studied here, some knee replacement models may have distinct stress concentrations and morphology differences as they interface with the native bone tissue. To accurately evaluate the effect of residual stress and shape distortions on the functionality of knee replacement, it is essential to take into account these specific design aspects. The residual stresses and shape distortions induced by the additive manufacturing process could cause implants to be weakened or warped. By incorporating more detailed and representative knee replacement models into simulation analyses, researchers can obtain a better understanding of how these implants interact with the adjacent bone tissue and evaluate the potential consequences for implant performance and patient outcomes.

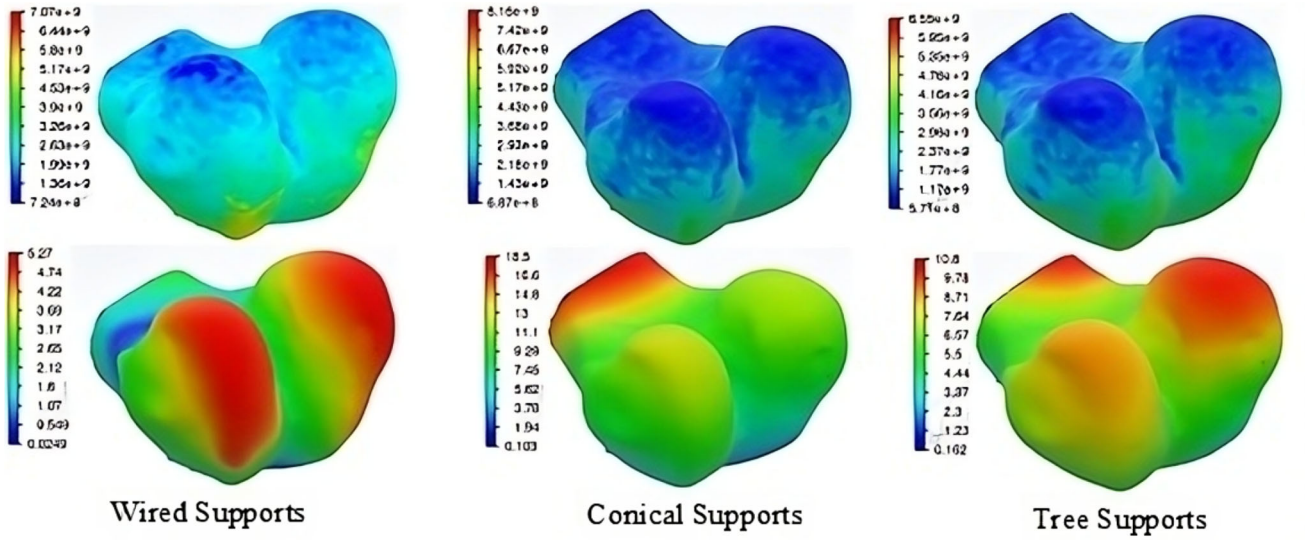

Fig. 11 Residual stress (top, unit: Pa) and part distortion (bottom, unit: mm) of the knee model, from AM simulations using three different types of support structures: wired or anchor (left), conical (middle), and tree (right)

In this study, we performed FE simulations to investigate the effects of AM process parameters, particularly build orientation and support structure, on shape distortion and residual stress formation. The proposed methodology can be employed to improve AM part quality (reduce residual stress and shape distortion) through simulation-guided optimization in AM process planning. We note that computationally intensive simulations would be needed for AM process optimizations, which involve a large number of simulation runs. Some data-driven surrogate modeling to replace physics-based intensive FE simulations could be useful in AM process optimizations [56–58], which will be considered in future research.

5 Conclusion

This study develops computed tomography (CT) image-based patient-specific finite element models (FEM) within a computational framework that helps to understand and decide the optimal build orientation and support structure for additive manufacturing (AM) knee replacements. A complete workflow has been built from CT images to 3D FEM and AM simulations, with image processing in open-source software 3DSlicer and MeshLab and AM simulations in commercial platform 3DEXPERIENCE. To demonstrate this approach, the workflow has been used to create a distal femur replacement for a 50-year-old male patient from the open-access Natural Knee Data (NKD) at Denver University. Mesh convergence studies were conducted to ensure reliable results. It was found that build orientations clearly affected both shape distortions and residual stresses. On the other hand, support structures have marginal influences on residual stresses but significantly impact shape distortions. Exploring how these manufacturing process planning parameters affect the residual stress and shape distortions that occur in AM can allow for the creation of AM products with improved part quality and performance. Future research can be performed on how residual stresses and shape distortions would affect the functionality of AM knee replacements during in-service physiological loading. More insights can be obtained by simulating other AM process parameters (layer thickness, hatch distance, laser power, scan speed, etc.) to evaluate their influences on AM knee replacements.

Table 5 Peak values of residual stress and shape distortion in AM knee model when varying support structures

Configuration	Max stress (GPa)	Max distortion (mm)
Anchor supports	7.07	5.27
Conical supports	8.16	18.5
Tree supports	6.55	10

We constructed a CT-FEM computational platform to find the optimal build orientation and support structure by running a number of finite element simulations. The maximum usage of open-source software (3DSlicer and MeshLab) from an open-access knee database to build up CT image-based patient-specific FEM knee models would be beneficial to promote the adoption of the developed workflow by researchers in the biomedical community. We note that experimental measurements of residual stresses and shape distortions on knee implants would be challenging, given the complicated geometries. Recently, a conformal-mapping-based discrete

uniformization method was developed for image registrations of complicated surfaces with high precision [54], which could be pursued in future research for experimental validations. Data-driven surrogate models can also be developed to replace the intensive FE simulations in the search for optimal AM process planning that minimizes shape distortions and residual stresses as outcomes. This study provides a computational platform for optimizing the configurations of AM processes for knee replacements, which will ultimately enhance the patient's quality of life using AM components.

Acknowledgements The assistance from Sarah Dulac and Alan Andonian was gratefully acknowledged.

Funding The authors gratefully acknowledged financial support provided by National Science Foundation (NSF) under grant number ACI-1548562 and CMMI-2309845.

Declarations

Conflict of interest The authors declare no competing interests.

References

1. Hanna Eskander HS (2016) Knee surgery: total knee replacement or partial knee replacement. Orthop Rheumatol 3(4). https://doi.org/10.19080/oroaj.2016.03.555619
2. Hériveaux Y, Le Cann S, Fraulob M, Vennat E, Nguyen V-H, Haïat G (2022) Mechanical micromodeling of stress-shielding at the bone-implant interphase under shear loading. Med Biol Eng Compu 60(11):3281–3293. https://doi.org/10.1007/s11517-022-02657-2
3. Hak DJ, Mauffrey C, Seligson D, Lindeque B (2014) Use of carbon-fiber-reinforced composite implants in orthopedic surgery. Orthopedics
4. Al-Tamimi AA, Peach C, Fernandes PR, Cseke A, Bartolo PJDS (2017) Topology optimization to reduce the stress shielding effect for orthopedic applications. Procedia CIRP 65:202–206. https://doi.org/10.1016/j.procir.2017.04.032. 3rd CIRP Conference on BioManufacturing
5. Al-Ketan O, Abu Al-Rub RK (2019) Multifunctional mechanical metamaterials based on triply periodic minimal surface lattices. Adv Eng Mater 21(10):1900524. https://doi.org/10.1002/adem.201900524
6. Bourell DL, Wohlers T (2020) Introduction to additive manufacturing. Addit Manuf Processes, 3–10. https://doi.org/10.31399/asm.hb.v24.a0006555
7. Balashanmugam N (2021) Perspectives on additive manufacturing in industry 4.0. Addit Manuf, 127–150. https://doi.org/10.1016/b978-0-12-822056-6.00001-1
8. Avila JD, Alrawahi Z, Bose S, Bandyopadhyay A (2020) Additively manufactured Ti6Al4V-Si-hydroxyapatite composites for articulating surfaces of load-bearing implants. Addit Manuf 34. https://doi.org/10.1016/j.addma.2020.101241
9. Melancon D, Bagheri ZS, Johnston RB, Liu L, Tanzer M, Pasini D (2017) Mechanical characterization of structurally porous biomaterials built via additive manufacturing: experiments, predictive models, and design maps for load-bearing bone replacement implants. Acta Biomater 63:350–368. https://doi.org/10.1016/j.actbio.2017.09.013
10. Gouge M, Michaleris P (2018) An introduction to additive manufacturing processes and their modeling challenges. Thermo-mechanical modeling of additive manufacturing, 3–18. https://doi.org/10.1016/b978-0-12-811820-7.00002-1
11. Feng Y (2021) Application of 3d printing technology in bone tissue engineering: a review. Curr Drug Deliv 18(2). https://doi.org/10.2174/18755704mtexxndcs2
12. Agarwal S, Darbar S, Saha S (2022) Application of additive manufacturing (am) technology in the medical field. Addit Manuf with Medical Applications, 223–232. https://doi.org/10.1201/9781003301066-12
13. Singh S, Ramakrishna S (2017) Biomedical applications of additive manufacturing: present and future. Curr Opin Biomed Eng 2:105–115. https://doi.org/10.1016/j.cobme.2017.05.006
14. Chua K, Khan I, Malhotra R, Zhu D (2021) Additive manufacturing and 3D printing of metallic biomaterials. Eng Regen 2:288–299. https://doi.org/10.1016/j.engreg.2021.11.002
15. Yuan L, Ding S, Wen C (2019) Additive manufacturing technology for porous metal implant applications and triple minimal surface structures: a review. Bioact Mater 4:56–70. https://doi.org/10.1016/j.bioactmat.2018.12.003
16. Zeng W, Lewicki KA, Chen Z, Van Citters DW (2021) The evaluation of reverse shoulder lateralization on deltoid forces and scapular fracture risk: a computational study. Med Nov Technol and Devices 11:100076. https://doi.org/10.1016/j.medntd.2021.100076
17. Williams K (1999) Finite element analysis for evaluating mechanical properties of the bone-implant interface. Mechanical Testing of Bone and the Bone-Implant Interface, 567–580. https://doi.org/10.1201/9781420073560.ch37
18. Hamed E, Novitskaya E, Li J, Jasiuk I, McKittrick J (2015) Experimentally-based multiscale model of the elastic moduli of bovine trabecular bone and its constituents. Mater Sci Eng: C 54:207–216. https://doi.org/10.1016/j.msec.2015.02.044
19. Biswas P, Guessasma S, Li J (2020) Numerical prediction of orthotropic elastic properties of 3D-printed materials using micro-CT and representative volume element. Acta Mech 231(2):503–516. https://doi.org/10.1007/s00707-019-02544-2. Accessed 09 Aug 2022
20. Watanabe K, Mutsuzaki H, Fukaya T, Aoyama T, Nakajima S, Sekine N, Mori K (2020) Development of a knee joint CT-FEM model in load response of the stance phase during walking using muscle exertion, motion analysis, and ground reaction force data. Medicina 56(2):56. https://doi.org/10.3390/medicina56020056
21. Jahadakbar A, Shayesteh Moghaddam N, Amerinatanzi A, Dean D, Karaca H, Elahinia M (2016) Finite element simulation and additive manufacturing of stiffness-matched niti fixation hardware for mandibular reconstruction surgery. Bioengineering 3(4):36. https://doi.org/10.3390/bioengineering3040036
22. Zhao D, Hart C, Weese NA, Rankin CM, Kuzma J, Day JB, Salary RR (2020) Experimental and computational analysis of the mechanical properties of biocompatible bone scaffolds, fabricated using fused deposition modeling additive manufacturing process. Volume 1: Additive Manufacturing; Advanced Materials Manufacturing; Biomanufacturing; Life Cycle Engineering; Manufacturing Equipment and Automation. https://doi.org/10.1115/msec2020-8511
23. Cheng L, Liang X, Bai J, Chen Q, Lemon J, To A (2019) On utilizing topology optimization to design support structure to prevent residual stress induced build failure in laser powder bed metal additive manufacturing. Addit Manuf 27:290–304. https://doi.org/10.1016/j.addma.2019.03.001
24. Beswick AD, Wylde V, Gooberman-Hill R, Blom A, Dieppe P (2012) What proportion of patients report long-term pain after total hip or knee replacement for osteoarthritis? A systematic review of prospective studies in unselected patients. BMJ Open 2(1). https://doi.org/10.1136/bmjopen-2011-000435

25. Ikeuchi M (2021) Chronic postsurgical pain after total knee arthroplasty. Pain Research 36(2):102–108. https://doi.org/10.11154/pain.36.102
26. Lifton J, Liu T (2021) An adaptive thresholding algorithm for porosity measurement of additively manufactured metal test samples via x-ray computed tomography. Addit Manuf 39:101899. https://doi.org/10.1016/j.addma.2021.101899
27. Harris MD, Cyr AJ, Ali AA, Fitzpatrick CK, Rullkoetter PJ, Maletsky LP, Shelburne KB (2016) A combined experimental and computational approach to subject-specific analysis of knee joint laxity. J Biomech Eng 138(8). https://doi.org/10.1115/1.4033882
28. Ali AA, Shalhoub SS, Cyr AJ, Fitzpatrick CK, Maletsky LP, Rullkoetter PJ, Shelburne KB (2016) Validation of predicted patellofemoral mechanics in a finite element model of the healthy and cruciate-deficient knee. J Biomech 49(2):302–309. https://doi.org/10.1016/j.jbiomech.2015.12.020
29. Bruns N (2019) 3D slicer. Der Unfallchirurg 122(8):662–663. https://doi.org/10.1007/s00113-019-0654-4
30. Cignoni P, Callieri M, Corsini M, Dellepiane M, Ganovelli F, Ranzuglia G (2008) MeshLab: an open-source mesh processing tool. In: Scarano V, Chiara RD, Erra U (eds) Eurographics Italian chapter conference. The Eurographics Association, ???. https://doi.org/10.2312/LocalChapterEvents/ItalChap/ItalianChapConf2008/129-136
31. Systemes D (2022) 3DEXPERIENCE user's guides. Dassault Systèmes, Waltham, MA, United States
32. Zhang Q, Xie J, London T, Griffiths D, Bhamji I, Oancea V (2019) Estimates of the mechanical properties of laser powder bed fusion Ti-6Al-4V parts using finite element models. Materials & Design 169. https://doi.org/10.1016/j.matdes.2019.107678
33. Huo Y, Lyu Y, Bosiakov S, Han F (2021) A critical review of the design, manufacture, and evaluation of bone joint replacements for bone repair. Materials 15(1):153. https://doi.org/10.3390/ma15010153
34. Zhang Q, Xie J, London T, Griffiths D, Bhamji I, Oancea V (2019) Estimates of the mechanical properties of laser powder bed fusion Ti-6Al-4V parts using finite element models. Materials & Design 169. https://doi.org/10.1016/j.matdes.2019.107678
35. Zhang Q, Xie J, London T, Griffiths D, Bhamji I, Oancea V (2019) Estimates of the mechanical properties of laser powder bed fusion Ti-6Al-4V parts using finite element models. Materials & Design 169. https://doi.org/10.1016/j.matdes.2019.107678
36. Anthony F (2019) Simple, example use of UEPACTIVATIONVOL in Abaqus for additive manufacturing simulation. Figshare software. https://doi.org/10.6084/m9.figshare.8279621.v1
37. London T, Bono DD, Oancea V, Tripathy S (2017) Predicting the properties of additively manufactured parts. Science in the Age of Experience
38. Zhang Q, Xie J, Gao Z, London T, Griffiths D, Oancea V (2019) A metallurgical phase transformation framework applied to SLM additive manufacturing processes. Materials & Design 166:107618. https://doi.org/10.1016/j.matdes.2019.107618
39. Zhang Q, Xie J, London T, Griffiths D, Bhamji I, Oancea V (2019) Estimates of the mechanical properties of laser powder bed fusion Ti-6Al-4V parts using finite element models. Materials & Design 169:107678. https://doi.org/10.1016/j.matdes.2019.107678
40. Zhang Y, Shapiro V (2018) Linear-time thermal simulation of as-manufactured fused deposition modeling components. J Manuf Sci Eng 140(7). https://doi.org/10.1115/1.4039556
41. Mohammadi M, Hematiyan MR (2021) Analysis of transient uncoupled thermoelastic problems involving moving point heat sources using the method of fundamental solutions. Eng Anal Boundary Elem 123:122–132. https://doi.org/10.1016/j.enganabound.2020.11.015
42. Daniyan I, Mpofu K, Oyesola M, Daniyan L (2020) Process optimization of additive manufacturing technology: a case evaluation for a manufactured railcar accessory. Procedia CIRP 95:89–96. https://doi.org/10.1016/j.procir.2020.01.143
43. Megahed S, Aniko V, Schleifenbaum JH (2022) Electron beam-melting and laser powder bed fusion of Ti6Al4V: transferability of process parameters. Metals 12(8):1332. https://doi.org/10.3390/met12081332
44. ABAQUS (2020) Standard User's Manual. Dassault Systemes Simulia Corp, Johnston, RI, USA
45. Vastola G, Zhang G, Pei QX, Zhang Y-W (2016) Controlling of residual stress in additive manufacturing of ti6al4v by finite element modeling. Addit Manuf 12:231–239. https://doi.org/10.1016/j.addma.2016.05.010
46. Cheng B, Chou K (2020) A numerical investigation of support structure designs for overhangs in powder bed electron beam additive manufacturing. J Manuf Process 49:187–195. https://doi.org/10.1016/j.jmapro.2019.11.018
47. Zhu L, Feng R, Li X, Xi J, Wei X (2019) A tree-shaped support structure for additive manufacturing generated by using a hybrid of particle swarm optimization and greedy algorithm. J Comput Inf Sci Eng 19(4). https://asmedigitalcollection.asme.org/computingengineering/article-pdf/19/4/041010/6598994/jcise_19_4_041010.pdf. https://doi.org/10.1115/1.4043530. 041010
48. ASTM (2020) Standard specification for wrought titanium-6aluminum-4vanadium alloy for surgical implant applications (uns r56400). ASTM International - Standards Worldwide
49. Kempen K, Yasa E, Thijs L, Kruth J-P, Van Humbeeck J (2011) Microstructure and mechanical properties of selective laser melted 18ni-300 steel. Phys Procedia 12:255–263. https://doi.org/10.1016/j.phpro.2011.03.033. Lasers in manufacturing 2011 - Proceedings of the sixth international WLT conference on lasers in manufacturing
50. Sun J, Yang Y, Wang D (2013) Parametric optimization of selective laser melting for forming ti6al4v samples by Taguchi method. Optics & Laser Technology 49:118–124. https://doi.org/10.1016/j.optlastec.2012.12.002
51. Denlinger ER, Heigel JC, Michaleris P, Palmer TA (2015) Effect of inter-layer dwell time on distortion and residual stress in additive manufacturing of titanium and nickel alloys. J Mater Process Technol 215:123–131. https://doi.org/10.1016/j.jmatprotec.2014.07.030
52. Wu AS, Brown DW, Kumar M, Gallegos GF, King WE (2014) An experimental investigation into additive manufacturing-induced residual stresses in 316L stainless steel. Metall and Mater Trans A 45(13):6260–6270. https://doi.org/10.1007/s11661-014-2549-x. Accessed 10 Jan 2023
53. Hodge NE, Ferencz RM, Vignes RM (2016) Experimental comparison of residual stresses for a thermomechanical model for the simulation of selective laser melting. Addit Manuf 12:159–168. https://doi.org/10.1016/j.addma.2016.05.011
54. Zhao J, Qi X, Wen C, Lei N, Gu X (2019) Automatic and robust skull registration based on discrete uniformization. In: 2019 IEEE/CVF International conference on computer vision (ICCV), pp 431–440. https://doi.org/10.1109/ICCV.2019.00052. ISSN: 2380-7504
55. Ryu J, Shrestha S, Manogharan G, Jung J (2018) Sliding contact wear damage of EBM built Ti6Al4V: influence of process induced anisotropic microstructure. Metals 8(2):131. https://doi.org/10.3390/met8020131
56. Aljarrah O, Li J, Huang W, Heryudono A, Bi J (2020) ARIMA-GMDH: a low-order integrated approach for predicting and optimizing the additive manufacturing process parameters. Int J Adv Manuf Technol 106(1):701–717. https://doi.org/10.1007/s00170-019-04315-8. Accessed 02 Sept 2020
57. Aljarrah O, Li J, Huang W, Heryudono A, Bi J (2019) A self-organizing evolutionary method to model and optimize correlated multiresponse metrics for additive manufacturing processes.

Smart Sustain Manuf Syst 3(2):20190024. https://doi.org/10.1520/SSMS20190024. Accessed 24 Jan 2022
58. Aljarrah O, Li J, Heryudono A, Huang W, Bi J (2022) Predicting part distortion field in additive manufacturing: a data-driven framework. J Intell Manuf. https://doi.org/10.1007/s10845-021-01902-z

Stephanie DeCarvalho received her Bachelor's Degree in Mechanical Engineering at the University of Massachusetts Dartmouth (2022). She is currently working on her Master's Degree in Mechanical Engineering at the University of Massachusetts Dartmouth. Her research is focused on the modeling of additively manufactured materials with biomedical applications.

Osama Aljarrah is an assistant professor of industrial and manufacturing engineering at Kettering University in Michigan. He earned a Master's degree in business administration from Yarmouk University and a Bachelor's degree in industrial & manufacturing engineering from Jordan University of Science and Technology. Aljarrah received his Ph.D. degree in industrial and systems engineering from the University of Massachusetts Dartmouth. Aljarrah joined Kettering University as an assistant professor after working in several industrial sectors. Surrogate modeling, evolutionary computing, simulation, and physics-informed machine learning are currently used in his research to determine how manufacturing process parameter variability affects additively manufactured components and the system behaviors.

Zi Chen is an Assistant Professor at Brigham and Women's Hospital and at Harvard Medical School. Dr. Chen received his bachelor's and master's degrees in Materials Science and Engineering from Shanghai Jiao Tong University and a Ph.D. in Mechanical and Aerospace Engineering from Princeton University. Before joining Brigham and Women's Hospital, Dr. Chen worked as an Assistant Professor at Dartmouth College and, before then, was a postdoctoral fellow in the Department of Biomedical Engineering at Washington University in St. Louis. Dr. Chen's research interests cover such diverse topics as soft robotics, mechanical instabilities of materials and structures, multistable structures, energy harvesting devices, biomimetic materials/devices, mechanics of morphogenesis, and cancer cell biomechanics. Dr. Chen's research has been supported by NIH, NSF, ONR, the Society in Science, and the American Academy of Mechanics. He has published 86 peer-reviewed papers in top journals such as Advanced Materials, Materials Today, PRL, Advanced Functional Materials, Small, EML, and APL, many of which were featured on the journals' cover and highlighted in media reports. Dr. Chen holds six patents and is a recipient of the Society in Science - Branco Weiss fellowship, the American Academy of Mechanics Founder's Award, and the International Association of Advanced Materials (IAAM) Innovation Award.

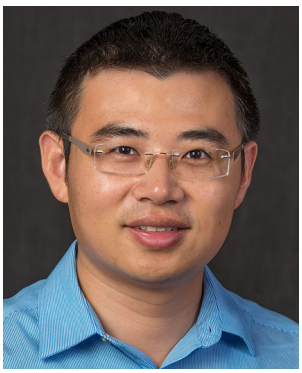

Jun Li is an assistant professor in Mechanical Engineering at the University of Massachusetts Dartmouth. He obtained his Ph.D. in Mechanical Engineering from the University of Illinois at Urbana-Champaign in 2012, where he also earned M.S. degrees in Mathematics and in Theoretical and Applied Mechanics. After that, he worked as a postdoctoral scholar in Aerospace at the California Institute of Technology and then as a quality assurance manager at Dassault Systemes SIMULIA before joining UMass Dartmouth in 2016. His research interest is in computational mechanics and materials in support of advanced manufacturing, energy, and biotechnology. He was the recipient of NASA RHG Exceptional Achievement for Engineering award in 2016 and the "Emerging Researchers in Biomedical Engineering" first-place award at the ASME International Mechanical Engineering Congress and Exposition in 2011.